Coupling GPR and ERT data interpretation to study the thermal imprint of a river in Syrdakh (Central Yakutia, Russia)

Albane Saintenoy, Marc Pessel, Christophe Grenier, Emmanuel Léger, Kencheeri Danilov, Kirill Bazhin, Ivan Khristoforov, Antoine Séjourné, Pasha Konstantinov

Coupling GPR and ERT data interpretation to study the thermal imprint of a river in Syrdakh (Central Yakutia, Russia)

Albane Saintenoy, Université Paris-Saclay, CNRS, GEOPS, 91405, Orsay, France*
Ivan Khristoforov, MPI, Yakutsk, Russia
Marc Pessel, Université Paris-Saclay, CNRS, GEOPS, 91405, Orsay, France
Christophe Grenier, LSCE, Gif-sur-Yvette, France
Emmanuel Léger, Université Paris-Saclay, CNRS, GEOPS, 91405, Orsay, France
Kencheeri Danilov, MPI, Yakutsk, Russia
Eric Pohl, LSCE, Gif-sur-Yvette, France
Kirill Bazhin, MPI, Yakutsk, Russia
Pavel Konstantinov, MPI, Yakutsk, Russia
Antoine Séjourné, Université Paris-Saclay, CNRS, GEOPS, 91405, Orsay, France

Summary

The thermal influence of a river on the surface conditions of a continuous permafrost in Yedoma sediments of Central Yakutia (Siberia, Russia) is studied by active layer (AL) thickness measurements along a cross section, CS9, with direct AL measurements (e.g. drilling), Ground-Penetrating Radar (GPR) and Electrical Resistivity Tomography (ERT) during late September 2017 and 2018. Reflections on the unfrozen/frozen interface when shallower than 2 m is detected on GPR data while ERT data inversion provides models of electrical resistivity down to 5 m. We study the effect of constraining ERT data inversion (using BERT software) with interface depth derived from GPR data and direct AL measurements, where available. The geophysical data enable us to reveal spatial variability in active layer depths, possibly related to river thermal influence. We compare our results with the 0°C isotherm obtained through simulating heat transfers with prescribed soil water content properties. We deduce a first estimate of the thermal imprint of the river.

Introduction

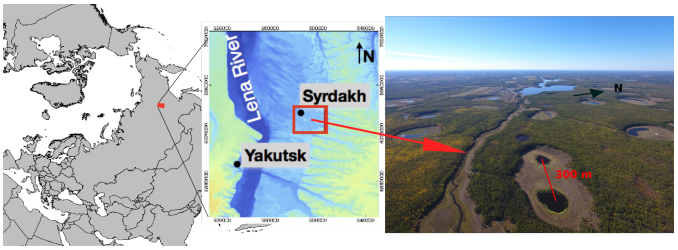

Fig. 1. Situation map of the site. The studied river is nearby Syrdakh village, 100 km North East of Yakutsk.

Fig. 2. Photography of the cross-section CS9.

The area of interest in Yakutia, is characterized by small rivers connecting thermokarstic lakes within Alas valleys (Fig. 1). Due to water latent heat effects, rivers influence soil below the riverbed compared to the surroundings. They influence the thermal equilibrium of the soil and the depth to permafrost in their vicinity. Here, we focus on a small river in a valley 100-km East of Yakutsk, close to Syrdakh village. The river is flowing from E to W, resulting in a S-facing right bank and a N-facing left bank, the latter largely covered with forest at the study site. The river width varies along its course from 2.5 m up to 15 m when the river forms larger water pools. In September 2017, exceptional conditions occurred because of two consecutive very dry years. As a result, the river mostly dried out and facilitated access to the riverbed, allowing us to use Ground-Penetrating Radar (GPR) and Electrical Resistivity Tomography (ERT) in order to measure detailed permafrost depth variations in one cross section, CS9, along the river (Fig. 2). Geophysical measurements were repeated in late September 2018, with this time about 40 cm of water at its deepest part.

Field geophysical experiments

GPR data were acquired using the Russian OKO system using two sets of antennas with nominal frequencies of 250 and 150 MHz. Trace interval is 5 cm and time window was adjusted depending on the antenna from 100 ns down to 300 ns.

Cross-section CS9 (Fig. 2) is equipped with 11 piezometers and 14 boreholes providing access to AL depth (i.e. the depth of the frozen/unfrozen interface). These measurements were used to calibrate geophysical data. In addition, four pits were dug after GPR data were acquired over a test profile. Diffraction hyperbolas analysis and adjusting depth measured in situ of the unfrozen/frozen interface with reflection arrival time observed on radargrams, gave an estimated electromagnetic wave velocity of 0.052 m/ns. All radargrams were migrated [1] using this velocity.

ERT data were acquired using a 16-channel instrument SibER-64 system with 64 electrodes and a 0.5-m spacing between electrodes, using Schlumberger and Wenner geometries. Data were inverted using the finite-element inversion program BERT to obtain the spatial distribution of soil electrical resistivity [2].

Results

A strong reflection appears on GPR data acquired late September 2017 (Fig. 3) and its depth is comparable to manual drilling estimations of the AL thickness. The river bed is in the topographic low zone, centered on 27.4 m from the beginning of the radargram. On the north side of the profile, the active layer was thicker (about 2 m) and no reflection is detectable on GPR data.

On ERT transects, the river bed is centered about 23 m from their beginning. The ERT data inversion gives an image of the electrical

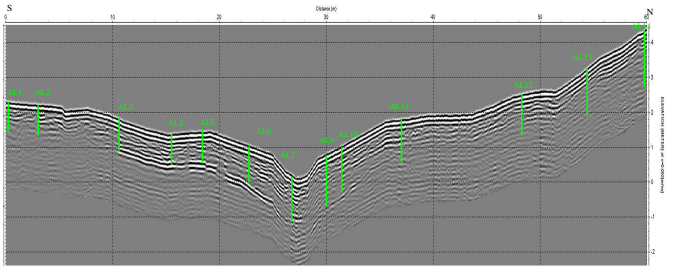

Fig. 3. GPR profile (250 MHz) acquired late September 2017 along CS9, with green vertical lines indicating active layer thickness measurements from drills.

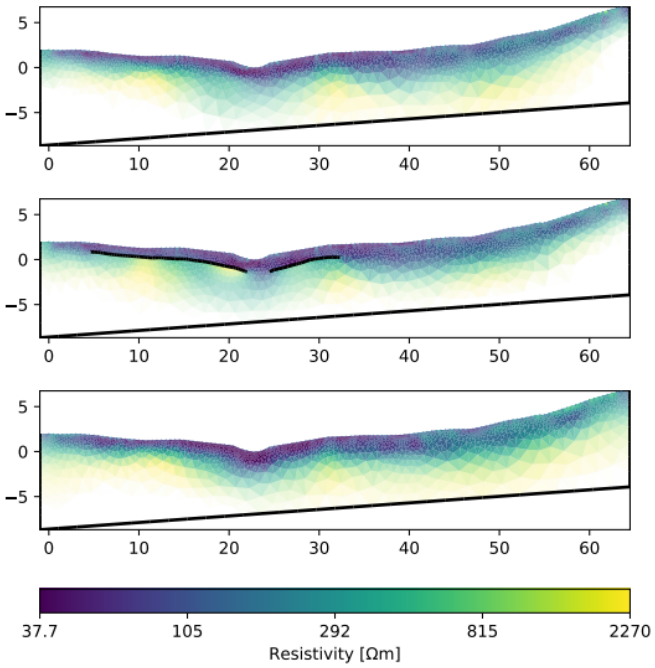

Fig. 4. Electrical resistivity model obtained from, top, 2017 ERT data inversion, middle, ERT data inversion constrained by an interface derived from GPR, and bottom, 2018 ERT data inversion.

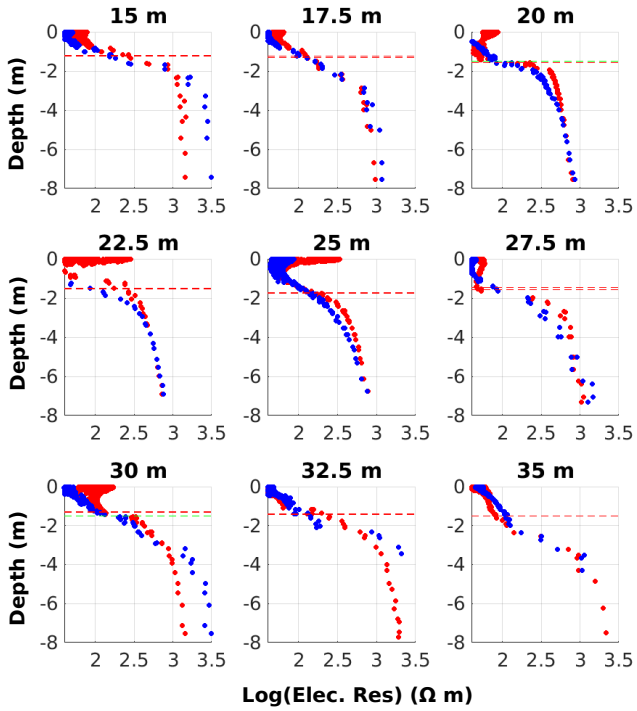

Fig. 5. Electrical resistivity vertical profiles across CS9 at different positions, from ERT data unconstrained inversion (red: 2017 data, and blue: 2018 data). The red dashed line is the depth of the reflector determined with GPR data from 2017. River bed is centered about 23 m from beginning of the profile.

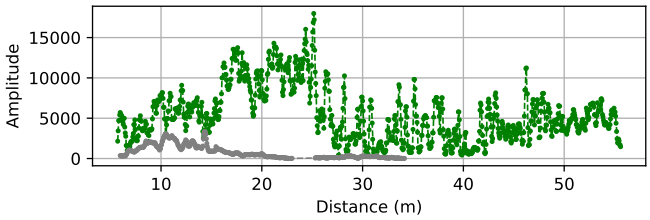

Fig. 6. GPR maximum amplitudes of the direct waves (green) and the reflection when visible (grey).

resistivity down to 5 m (top of Fig. 4), showing some vertical variations that are consistent with expected electrical response: active layer (above isotherm 0°C) should have an electrical resistivity lower than the one of permafrost. For example, at an Alaskan site [3], resistivity values below 400Ωm, are interpreted as corresponding to unfrozen conditions, while values above 400 Ωm were interpreted to correspond to frozen or partially frozen.

Including an interface at the depth derived from GPR data in the ERT data inversion process [4], gives the image in the middle of Fig. 4. This second model is imaging a lower resistivity zone above the GPR interface with some lateral variations. The constrained inversion helps to better define the active layer limits, but further studies on sensitivity analysis are currently carried on.

To highlight the links between electrical resistivity and permafrost position, we derived electrical resistivity vertical profiles from the inverted ERT transects (Fig. 4). The obtained electrical resistivity vertical profiles are displayed in Fig. 5. On each vertical profiles, the depth of the interface derived from 2017 GPR data is indicated as a red dashed line. The interface seems to be related to the inflection point of the red curves from 2017 ERT data. This behaviour is similar to the one observed for GPR reflections, linked to water table positions [5].

Looking at the vertical profiles from the 2017 data ERT (red points), the effect of the river (centered about 23 m) is clearly visible on the electrical resistivity deeper that the AL depth. At 15 m and after 30 m the electrical resistivity is higher than 1000 Ωm, while below the river it is less than 1000 Ωm. This difference could be explained by temperature differences in the top part of the permafrost [6], the high water content of the river zone creating warmer temperature underneath.

In the AL, variability in electrical resistivity is visible and can be related to the amplitudes of the GPR direct waves along the profile (Fig. 6). In between 18 and 28 m from the beginning of the profile, the amplitude of the direct wave is on average 2 times higher than elsewhere on the profile. In this interval, resistivity vertical profiles

show a high value on the surface then a decrease before increasing again to its value about 1000 Ωm.

These two facts should be related as the intensity of the ground wave is directly influenced by the immediate surrounding electrical resistivity and dielectric permittivity. After 32 m the amplitude of the direct wave is reduced and the AL is thicker, impeaching any GPR reflection detection on the radargram.

Finally, differences in between 2017 and 2018 ERT models below the AL depends on the distance from the river. When more than about 6 m away from the river bed center (15 and 17.5 m on south bank and 30, 32.5 and 35 m on north bank), the electrical resistivity below the AL is systematically higher in 2018 than in 2017. Relating electrical resistivity value to temperature, it could mean that the top part of the permafrost on these locations are more sensitive to air temperature changes. At the opposite, in the proximity of the river and underneath, the high water content zone is acting as a buffer zone and limiting difference from one year to the other.

In the idea of testing our hypothesis we present heat transfer numerical simulations.

Heat transfer numerical experiment

In a preliminary approach, the system evolution was simulated by means of Cast3M code [7], http://www-cast3m.cea.fr, representing heat transfers only with prescribed soil water content properties. The modelled system geometry is a 2D transect centered on the river and extending to 20 m depth and into the valley transverse to the river. Boundary conditions are imposed geothermal flux at the bottom, zero heat flux on the sides and imposed temperature on the top of the mesh. These surface conditions result from air temperature measurements at the nearest meteorological station (Yakutsk City). An average year over the whole Syrdakh field monitoring period (2012-2019) is computed and transferred into soil temperature considering transfer functions obtained from air temperature and soil temperature in situ monitoring at 10 cm depth. The river sediment temperature and south oriented vs north oriented slopes temperatures provide spatially variable temperature boundary conditions at the top of the modelled system. A spin up on this average year was computed until convergence to steady state conditions are obtained. Some minor calibration was made to match temperature measurements available at different distances from the river along the CS9 transect (4 series of monitoring distances with measurement depths of 1, 2, 3 and 4 meters and a 4 measurement departs below river at 30 cm, 1.2 m, 2. and 3. meters). This calibrated average year provided the time evolution of the whole simulated 2D system throughout this average year (Fig. 7. The 0°C isotherm depth was then extracted for the 15th of September to provide the ALD to be compared with field measurements (Fig. 8).

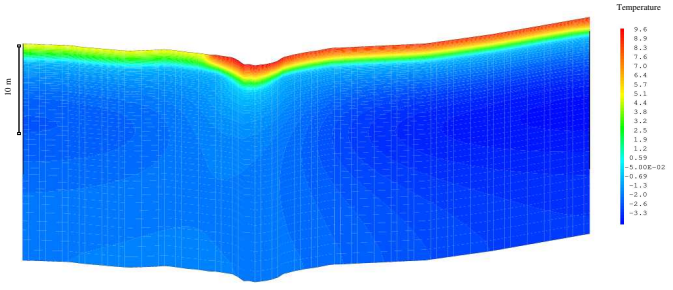

Fig. 7. Temperature distribution calculated with heat transfer modeling code with imposed surface temperature.

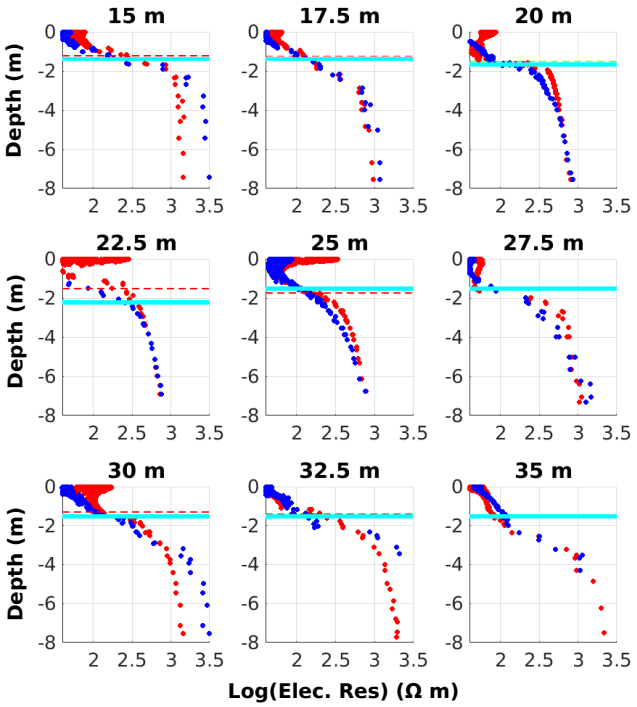

Fig. 8. Adding in light blue the position of the isotherm $0°C$ on the electrical resistivity profiles of Fig. 5.

Discussion

The comparison of GPR, ERT and heat transfer simulations are rising many questions that need more work to be answered precisely. However, at a first glance, these three methods give ideas of interaction between a small river, the AL thickness, its evolution and its influence on the top permafrost temperature. The cross section studied here, shows that a 2.5 m width river bed is thermally influencing a 12 m width zone underneath. The same analysis carried out on another CS where the river is wider (about 8 m) is currently going on and confirms our interpretations.

Acknowledgments

We gratefully acknowledge funding from Univ. Paris-Saclay SPU Carbon Fate Emerging Project, Labex-IPSL and RFBR grants N16-31-60082-mol-a-dk and the help of Frédéric Bouchard on the field.

References

[1] R. Stolt, "Migration by fourier transform," *Geophysics*, vol. 43, no. 1, pp. 23–48, 1978.

[2] C. Rücker, T. Günther, and F. M. Wagner, "pygimli: An open-source library for modelling and inversion in geophysics," *Computers & Geosciences*, vol. 109, pp. 106–123, 2017.

[3] B. Dafflon, R. Oktem, J. Peterson, C. Ulrich, A. P. Tran, V. Romanovsky, and S. S. Hubbard, "Coincident aboveground and belowground autonomous monitoring to quantify covariability in permafrost, soil, and vegetation properties in arctic tundra," *Journal of Geophysical Research: Biogeosciences*, vol. 122, no. 6, pp. 1321–1342, 2017.

[4] E. Léger, B. Dafflon, F. Soom, J. Peterson, C. Ulrich, and S. Hubbard, "Quantification of arctic soil and permafrost properties using ground-penetrating radar and electrical resistivity tomography datasets," *IEEE Journal of Selected Topics in Applied Earth Observations and Remote Sensing*, vol. 10, no. 10, pp. 4348–4359, 2017.

[5] A. Saintenoy and J. W. Hopmans, "Ground Penetrating Radar: Water table detection sensitivity to soil water retention properties," *IEEE Journal of Selected Topics in Applied Earth Observations and Remote Sensing (IF 1.489)*, vol. 4, pp. 748–753, 2011.

[6] E. Léger, B. Dafflon, Y. Robert, C. Ulrich, J. E. Peterson, S. C. Biraud, V. E. Romanovsky, and S. S. Hubbard, "A distributed temperature profiling method for assessing spatial variability in ground," *The Cryosphere*, vol. 13, p. 11, 2019.

[7] C. Grenier, H. Anbergen, V. Bense, Q. Chanzy, E. Coon, N. Collier, F. Costard, M. Ferry, A. Frampton, J. Frederick, *et al.*, "Groundwater flow and heat transport for systems undergoing freeze-thaw: Intercomparison of numerical simulators for 2d test cases," *Advances in water resources*, vol. 114, pp. 196–218, 2018.